E1-2017-20

L. Glonti, T. Enik, V. Kekelidze, A. Kolesnikov,
D. Madigozhin, N. Molokanova, S. Movchan,
Yu. Potrebenikov, S. Shkarovskiy

LONGITUDINAL TENSION AND MECHANICAL STABILITY OF A PRESSURIZED STRAW TUBE

Submitted to “Nuclear Instruments and Methods in Physics Research”

Глонти Л. и др. Е1-2017-20
Продольное натяжение и механическая устойчивость
тонкостенной дрейфовой трубки под давлением

При разработке детекторов заряженных частиц на основе тонкостенных дрейфовых трубок (строу), работающих в вакууме, необходима техника оценки их механических свойств. В настоящей работе представлен экспериментальный метод изучения свойств натянутых длинных строу-трубок, находящихся под внутренним давлением. Результаты выполненных измерений в основном согласуются с расчетами в низшем приближении с учетом известных значений и неопределенностей параметров материала трубок. Показано, что эффективное натяжение трубки, равное разности между полным продольным натяжением ее стенки и силой давления в расчете на ее поперечное сечение, определяет поперечную устойчивость трубки и низшую частоту ее колебаний. Это может быть основой нового метода контроля механических свойств действующей дрейфовой трубки.

Работа выполнена в Лаборатории физики высоких энергий им. В. И. Векслера и А. М. Балдина ОИЯИ.

Препринт Объединенного института ядерных исследований. Дубна, 2017

Glonti L. et al. E1-2017-20
Longitudinal Tension and Mechanical Stability
of a Pressurized Straw Tube

When developing charged particle detectors based on straw tubes working in vacuum, a special technique is needed for their mechanical properties evaluation. An experimental method of strained pressurized straw tube mechanical properties study is presented. The performed measurement results are in agreement with the approximate calculations taking into account the known uncertainties of the wall material parameters. It is shown that the difference between the tube wall longitudinal tension and the pressure force applied to the tube cross section area defines both the straw tube transverse stability and the lowest value of its oscillation frequency.

The investigation has been performed at the Veksler and Baldin Laboratory of High Energy Physics, JINR.

Preprint of the Joint Institute for Nuclear Research. Dubna, 2017

INTRODUCTION

During the last decades, a series of experiments in high energy physics have been designed in order to investigate very rare decay modes that require precision measurement of charged particles momenta and positions (see, for example, [1, 2]. It stimulates further development of gaseous particle detectors based on straw tubes (straw trackers) containing gas under pressure (typically under atmospheric one) and working in vacuum. In particular, the purpose of NA62 experiment [1] is to measure $K^+ \to \pi^+ \nu\bar{\nu}$ decay branching ratio, that requires an unprecedented precision of charged pion momentum measurement.

The problem of straw tubes strength and stability becomes especially important when drift tubes of particle detectors are placed into vacuum in order to minimize the multiple scattering of detected particles. In such a case, both the filling gas pressure P and the external longitudinal tension force T are applied simultaneously, and their combined effect should be understood at least in the simplest approximation.

Only two coordinate directions related to straw tube geometry are essential for the problem of a strained straw under pressure: the axial direction along the straw axis ($\|$) and the circumferential direction ($\perp$) tangent to the straw cylindrical surface in the plane normal to the axis. Radial dependence of wall stress is negligible when the straw wall thickness h is much smaller than the straw radius R.

For a pressurized tube with a very thin wall glued into a rigid frame by means of a rigid plug, one can derive an approximate equation for the radius as a function of distance Z from the gluing place:

$$\frac{TR''}{2\pi} - Eh\left(\frac{R}{R_0} - 1\right) + PR = 0, \tag{1}$$

where E is the wall Young's module and R_0 is the nominal straw radius that remains fixed at the end glued into the frame. The first term of (1) represents a force that is caused by the wall longitudinal curvature, the second one is an effect of circumferential stress, and the last term is a pressure effect. The solution satisfying the boundary condition $R(0) = R_0$ is

$$R = R_0 + \frac{PR_0^2}{Eh - PR_0}\left(1 - \mathrm{e}^{-Z\sqrt{2\pi(Eh/R_0 - P)/T}}\right). \tag{2}$$

For the typical straw characteristics (see below) one can calculate that a usual radius transition zone is much shorter (of the order of 1 mm) than a typical straw length L of 2 m. So we can ignore the presence of the transition zone and assume that the straw radius is uniformly increased by the applied pressure for the complete straw tube. Also, one can show that the pressure force applied to the end plug may be calculated for the increased radius $R(\infty)$ in order to take into account the axial component of the pressure applied to the transition zone, that otherwise should be subtracted from the axial wall tension applied to the plug.

Straw circumferential (hoop) stress caused by the inner pressure P can be evaluated as [3]

$$\sigma_\perp = \frac{PR}{h}. \tag{3}$$

This is a general relation for a straw with inner pressure, as no other forces appear in transverse directions (circumferential or radial). However, R in (3) may be deviated from R_0 due to the pressure and tension effects.

Straw axial stress may be caused by different reasons depending on the conditions at the ends. For example, if the pressure acts not only on the cylindrical shell but also on the free ends closed by airtight end plugs, one can write a simple relation between hoop and axial stress values:

$$\sigma_\parallel^P = \frac{P\pi R^2}{2\pi Rh} = \frac{PR}{2h} = \frac{\sigma_\perp}{2}. \tag{4}$$

Hoop stress leads to the transverse strain for straw cross section perimeter defining the first contribution to the radius relative change: $\epsilon_\perp^1 = \Delta R^1/R = \sigma_\perp/E = PR/Eh$. As a consequence, the Poisson effect gives a negative contribution to the axial strain: $\epsilon_\parallel^R = \Delta L^R/L = -\mu(\Delta R/R) = -\mu(PR/Eh)$. It is added to the other contribution to elongation $\epsilon_\parallel^1 = \sigma_\parallel^P/E$ caused by the pressure force applied to the end plugs. A similar derivation may be done for the hoop strain, also taking into account the Poisson effect. So for a straw with free closed ends we have

$$\epsilon_\parallel = \frac{PR}{2hE}(1 - 2\mu), \tag{5}$$

$$\epsilon_\perp = \frac{PR}{2hE}(2 - \mu). \tag{6}$$

In [4], the straw elongation according to formula (5) has been studied, and it is found to be precise enough within our knowledge about the material properties.

The hoop strain formula (6) has been derived for the pressure vessel example in [3].

But in the typical experimental setup exploiting straws in vacuum (like [1]), the straw ends are fixed by means of gluing into the rigid frame. In this case, the above formulae are irrelevant, as the pressure force applied to the fixed end plug is compensated by the rigid frame rather than by the axial stress of the tube. Moreover, the end plug with a gas supply channel even does not feel any pressure force, as the pressures inside the straw and behind the plug are equalized.

Usually it is difficult to investigate the straw mechanical state when the tube ends are glued into the rigid frame, as in this case no directly measurable straw characteristics like elongation or individual straw tension are easily available. So one needs an auxiliary installation for this purpose.

1. TESTBENCH FOR STUDIES OF A STRAINED STRAW UNDER PRESSURE

A special testbench (see Fig. 1) has been built in order to study straw mechanical properties under the inner pressure excess that simulates an effect of vacuum outside the straw in some real particle detector setup. The testbench is used in order to test straws subjected to both a preliminary external tension T_0 and an inner pressure excess P (that is applied afterwards). The resulting longitudinal force applied to straw T_P is measured by means of tensometer Tm based on the single-point aluminium load cell (Tedea-Huntleigh, model 1022) [5] with a maximum measured force of 10 kgf.

A straw specimen is closed on the tensometer side by the end plug $e1$ with the end cap C using glue for rigid sealing. End cap C is connected with the tensometer Tm by means of two flexible joints and a rigid rod. The other straw end contains a plug $e2$ with a gas supply channel. This straw end is glued into the solid support that may be moved along the rigid basement B and fixed on a specific place in order to create a preliminary straw tension prior to the test.

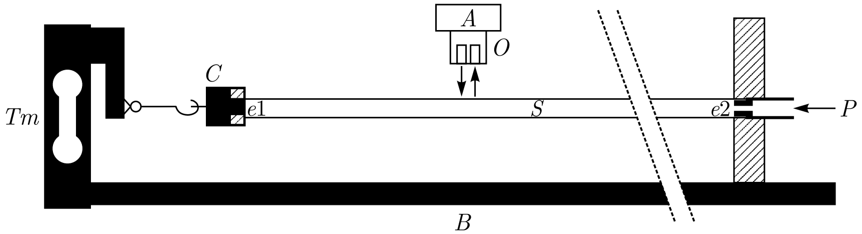

Fig. 1. The testbench scheme: B — rigid basement; Tm — tensometer; $e1$ — closed end plug; $e2$ — end plug with a gas supply channel; C — end cap with a sealing; P — pressure supply; S — straw; O — optical coupler; A — amplifier

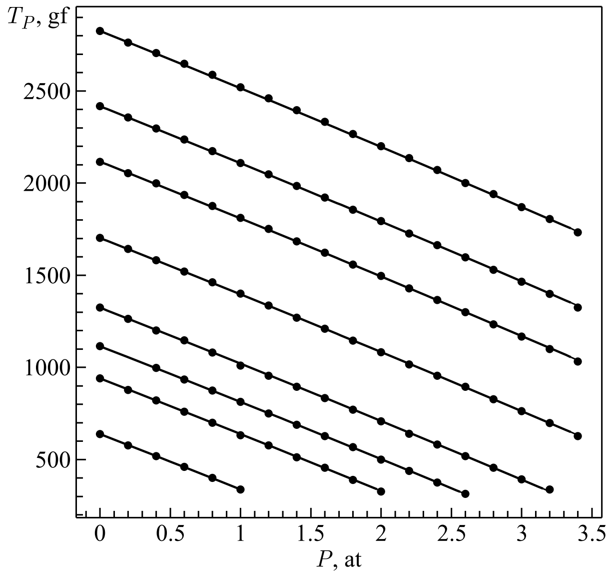

Fig. 2. Straw effective tensions T_P versus the pressure excess P for the different initial tensions $T_P(0)$ for the straw A. Circles — measurements; solid lines — result of the fit by formula (12) with a common set of fit parameters

Then the pressure supply is opened, and the changing pressure values P(at) are recorded together with the corresponding values of tensometer measurements T_P (in gf) (see experimental points in Figs. 2 and 3, a).

Straw oscillations are studied by means of the optical coupler O (see Fig. 1) that emits constant intensity infrared radiation and registers the radiation reflected from the straw wall. When the straw oscillations are mechanically excited, the registered radiation intensity is modulated by the changing distance to the wall. The obtained signal is amplified and sent to the oscilloscope with a Fast Fourier Transform function. In the resulting frequency spectrum the lowest peak position is regarded as a straw lowest frequency.

In general, end cap C may be shifted down due to its weight of $10 - 20$ gf. But for the horizontal force $T_P > 300$ gf (assuming the cap weight of 25 gf) it has been estimated that the cup vertical shift is below 4 mm. It leads to the relative elongation of two-meter straw at the level of 10^{-4}, that is much less than the minimum straw elongation caused by the preliminary tension (10^{-3}). So the straw ends may be considered as the fixed ones after the application of preliminary tension. For $T_P < 300$ gf, the condition of fixed straw ends may be violated, and for a limit of free straw ends the measured T_P on the testbench is defined mainly by the cap weight.

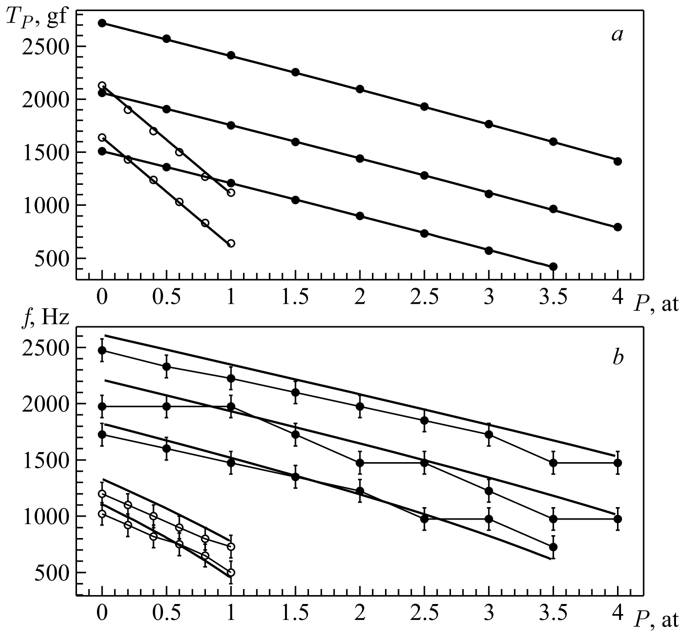

Fig. 3. a) Straw effective tensions T_P versus the pressure excess P for the different initial tensions $T_P(0)$; b) straw lowest oscillation frequency for the corresponding T_P and P. Filled circles — straw A, open circles — straw B (see the text). Solid curves — calculations with the $\mu_\perp(E_\parallel/E_\perp)$ and k values from the Table. Error bars represent an estimation of uncertainty (1 Hz) for the frequency measurement

Straw example properties and measurement results

Property	Straw A	Straw B
Diameter, mm	9.8	18.0
Length, m	2.1	1.9
Wall thickness, μm	36	54.44
Linear density, g/m	1.55	4.31
$E_\parallel$, N/mm^2 [6]	4500	4000
$E_\perp$, N/mm^2 [6]	5000	5500
k, μm$^2/N$	4.0 ± 0.5	-2.9 ± 14.5
$\mu_\perp(E_\parallel/E_\perp)$	0.305 ± 0.016	0.296 ± 0.020
$\mu_\perp$	0.34 ± 0.04	0.41 ± 0.04

Two straw specimens have been tested (see the Table). The first one (straw A) is the NA62 straw with the length of 2.1 m. It has been produced at the Joint Institute for Nuclear Research (Dubna) together with nearly 7000 straws mounted in the NA62 Spectrometer [1]. The tubes are made of 36 μm thin polyethylene terephthalate (PET) foils (Hostaphan® [6]), coated inside the tube with two thin metal layers (0.05 μm of Cu and 0.02 μm of Au) in order to provide electrical conductivity on the cathode and to improve the straw tube gas impermeability. The material density of 1.4 g/cm^3 [6] was used to estimate the straw A linear density from its radius and wall thickness.

The second tube specimen (straw B) is the straw 18 mm in diameter made of more thick Hostaphan® film. For the specimen B, a linear density has been measured by means of weighting (with the result of 4.31(6) g/m), as the wall thickness is not strictly defined in the film specification.

2. STRAW EFFECTIVE TENSION CALCULATION AND MEASUREMENT

Hostaphan® producer reports quite different values for the transverse (Transverse Direction, TD) and longitudinal (Machine Direction, MD) Young's moduli [6] (see the Table). So the film material is not isotropic due to the sophisticated production process, and we should distinguish the transverse (hoop) and longitudinal (axial) straw properties. In particular, the first contribution to the transverse relative radius change is $\epsilon_\perp^1 = \Delta R^1/R = \sigma_\perp/E_\perp = PR/(E_\perp h)$.

Due to the Poisson effect, the hoop strain causes an axial strain of the opposite sign, so the straw would become shorter if the ends were not fixed. This virtual small relative change of length is

$$\epsilon_\parallel^R = \frac{\Delta L^R}{L} = -\mu_\perp \frac{\Delta R^1}{R} = -\mu_\perp \frac{PR}{(E_\perp h)},$$

where $\mu_\perp$ is the transverse Poisson's ratio for the loading applied transversely with respect to the straw axis.

But in our case the straw ends are fixed, that means an appearance of compensatory tension force ΔT (and corresponding axial stress $\Delta T/(2\pi Rh)$) that returns straw length to its initial value

$$\frac{\Delta T}{2\pi Rh} = E_\parallel \frac{\Delta L^R}{L} = \mu_\perp P \frac{R}{h} \frac{E_\parallel}{E_\perp}. \tag{7}$$

So we have an additional straw wall axial tension caused by the supplied pressure $\Delta T = \mu_\perp (E_\parallel/E_\perp) P 2\pi R^2$.

But on the present testbench the value measured by tensometer is an effective tension T_P, that is, the straw wall tension minus the pressure force applied to the end plug from inside of the straw:

$$T_P = T_0 + 2\mu_\perp \frac{E_\parallel}{E_\perp} P\pi R^2 - P\pi R^2 = T_0 - \left(1 - 2\mu_\perp \frac{E_\parallel}{E_\perp}\right) P\pi R^2. \tag{8}$$

We know that Poisson's ratio μ for plastics is typically less than 0.5, so in total the increase of straw pressure leads to the decreasing of measured T_P in spite of the true straw tension T growth

$$T = T_0 + \Delta T = T_0 + 2\mu_\perp \frac{E_\|}{E_\perp} P\pi R^2. \tag{9}$$

For a particle detector like NA62 Spectrometer [1], one can calculate the full force applied to the frame by a gas-filled straw using (8), if the effect of external atmospheric pressure applied to the frame is calculated just ignoring all the holes made for the straws. In such a case, the true wall tension value (9) is needed only to control the straw tensile strength.

One could note that on the present testbench the special case of zero effective tension ($T_P = 0$) means that straw ends are free. As mentioned above, in these conditions (for $T_P < 300$ gf) the fixed-ends formulae become irrelevant for the given testbench due to gravitation effect. Nevertheless, just in order to check the formulae consistency we can derive a free-ends straw elongation using $T_P = 0$ condition. From (8) for this case $T_0 = (1 - 2\mu_\perp(E_\|/E_\perp))P\pi R^2$. Initial elongation of the fixed straw due to the preliminary tension T_0 is equal to free straw elongation under the pressure, ensuring $T_P = 0$ for the fixed-ends straw. So for the free straw ends we have

$$\frac{\Delta L}{L} = \frac{T_0}{E_\| 2\pi R h} = \left(1 - 2\mu_\perp \frac{E_\|}{E_\perp}\right) \frac{PR}{(2E_\| h)},$$

that is equivalent to (5) for isotropic material.

Finally, a small correction for the straw radius change is taken into account. Two effects contribute to the straw radius change on the testbench. One term is the radius relative decrease due to the initial axial tension applied: $\Delta R^L/R = -\mu_\| \Delta L/L = -\mu_\| T_0/E_\| 2\pi R h$, where $\mu_\|$ is the longitudinal Poisson's ratio defined for the loading along the straw axis.

Another term is the radius relative increase due to the pressure applied from inside. First-order effect is just $\sigma_\perp/E_\perp = PR/E_\perp h$, but if one takes into account the additional tension applied from the fixed ends that compensates the tube shortening which could be caused by the radius increase, the term becomes $(1 - \mu_\| \mu_\perp)(PR/E_\perp h)$. So the radius dependence on pressure and initial tension looks like

$$R = R_0 \left(1 + (1 - \mu_\| \mu_\perp)\frac{PR_0}{E_\perp h} - \frac{\mu_\| T_0}{E_\| 2\pi R_0 h}\right). \tag{10}$$

For this small correction we will assume $\mu_\| = \mu_\perp$, but we should remember that in the main formula (8) we have a transverse Poisson's ratio.

It is known that any material becomes nonlinear with respect to large applied force, while the material linear properties are defined for zero-force limit. But on the testbench a precision measurement becomes problematic for the low effective tensions T_P. So we need to take into account the possible nonlinearity in such a way that the resulting $\mu_\perp$ could be easily extracted for the limit of low wall tension and low pressure.

For this purpose, we can postulate a weak linear dependence of Poisson's ratio as a function of transverse stress. We introduce the value

$$\nu = \mu_\perp \frac{E_\parallel}{E_\perp} - \frac{kT}{2\pi Rh} \tag{11}$$

instead of just $\mu_\perp(E_\parallel/E_\perp)$ into all the related expressions. Apart from the real material nonlinearity, k coefficient also absorbs an effect of small setup deformation under tension as well as next-order effects ignored in the formulae. So the coefficient is regarded here as a technical value that vanishes from the final result for $T = 0$.

But T and R entering (11) in turn depend on the running Poisson's ratio value. So we implement an iterative approach starting with a tension $T = T_0$, nominal straw radius $R = R_0$, and the starting Poisson's ratio value of $\nu = \mu_\perp(E_\parallel/E_\perp)$. On each iteration new T, ν, R values were calculated, three iterations were quite enough for the calculation precision.

We have two free parameters ($\mu_\perp(E_\parallel/E_\perp)$ and k), that is enough to describe our data on the measured tensions and pressures. Figure 2 shows the measured effective tensions for the NA62 straw together with the result of their fit with the formula

$$T_P = T_0 - (1 - 2\nu)P\pi R^2. \tag{12}$$

MINUIT [7] package called from ROOT [8] interface has been used in order to obtain the resulting fit parameter values and their fit errors.

The fit is done with the same assumed error for all the experimentally measured T_P values related to the given straw. These measured errors (straw A: $\pm$3.6 gf, straw B: $\pm$20.47 gf) are defined in such a way that a resulting $\chi^2/ndf = 1$ in order to obtain some sensible fit errors that are considered as the statistical uncertainties for the extracted free parameters.

Straw A two-parameter fit results are: $\mu_\perp(E_\parallel/E_\perp) = 0.3051 \pm 0.0005_{\text{stat}}$; $k = (3.98 \pm 0.16_{\text{stat}})$ μm$^2/N$. Fit results for the straw B are: $\mu_\perp(E_\parallel/E_\perp) = 0.2961 \pm 0.0150_{\text{stat}}$; $k = (-2.89 \pm 14.34_{\text{stat}})$ μm$^2/N$. So for the second specimen the nonzero term k presence is not confirmed, may be due to the limited available interval of measured tensions and pressures in this case.

The systematic uncertainty due to the limited knowledge of Young's moduli with a fixed ratio $E_\parallel/E_\perp$ is estimated as the effect of the radius correction (10) removal that corresponds to the limit of infinitely large Young's moduli. Almost the same absolute change of the results (in opposite direction) is caused by the halving of both $E_\parallel$ and $E_\perp$ in (10), so we take the largest change (related to the radius correction switching off) as the contribution to the systematic error.

The Gaussian width of the NA62 straw diameter distribution can be estimated as 0.03 mm, and the systematic shift of the central value from the nominal number may have the same size [1]. So taking conservatively the possible diameter systematic uncertainty of 0.1 mm for the tested specimens, we have obtained the radius related contribution to systematic error.

Apart from that, an effect of 5% systematic scale change both in the measured effective tension and pressure are taken as independent contributions to the systematic errors.

Combining all the above statistic and systematic contributions in quadrature, we have finally the $\mu_\perp(E_\parallel/E_\perp)$ results shown in the Table. Taking into account the producer's information about Young's moduli ratio, we extract the $\mu_\perp$ central values shown in the Table. Finally, $\mu_\perp$ uncertainties depend essentially on the moduli errors that may be roughly estimated from the provided significant digits: $\delta(E_\perp/E_\parallel) \approx 0.1$.

Typically, the reported longitudinal Poisson's ratio values $\mu_\parallel$ for oriented PET films are 0.37–0.44 [9, 10], so the obtained transverse Poisson's ratios look reasonable in comparison with the usually measured longitudinal ones.

Results of the effective tension comparison for the two straw specimens are shown in Fig. 3, *a*. The observed strong dependence of $T_P(P)$ slope on the straw radius is well reproduced by formula (12).

3. TRANSVERSE STABILITY AND OSCILLATIONS OF THE STRAINED STRAW UNDER PRESSURE

Let us consider a very short cylindrical element of an almost straight tube (Fig. 4) limited by its two cross sections. If a small curvature appears, in the first approximation all the local cross sections conserve their shape and slightly rotate to remain perpendicular with respect to the curved tube axis. The total longitudinal tension $|T_{AB}| = |T_{CD}| = |T|$ remains almost stable in spite of the stress difference on the tube sides.

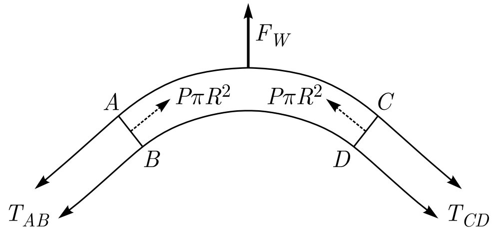

Fig. 4. Forces applied to the curved tube element subjected both to inner pressure and axial tension

But the area of the arched side of the wall (upper side in Fig. 4) becomes larger than the area of the concave part (lower side in the same figure) due to the wall extension and compression. As a result, the summary nonzero pressure force applied to the wall F_W appears, that is directed towards the arched side of the wall. So the pressure excess in the tube always tries to increase the tube curvature.

In order to estimate F_W, let us imagine an absolutely rigid shell that consists of the curved cylinder-like wall with two additional transverse plugs that close tightly the cross sections AB and CD. A summary force applied by inner pressure to the closed rigid shell is always zero. So the total pressure force applied to the curved wall is equal, with the opposite sign, to the vector sum of pressure forces applied to the end plugs.

Returning to the soft tube element, one can conclude that the pressure force F_W applied to the wall of the element is equal to the vector sum of two forces $P\pi R^2$, each of them is directed against T_{AB} or T_{CD} which are not collinear.

So the transverse dynamics of the curved tube element is defined by the difference between the wall longitudinal tension and the $P\pi R^2$ term, that is the effective tension (8) to be measured on the testbench described above.

The straw curvature tends to eliminate itself only for the positive effective tension $T_P = (T - P\pi R^2) > 0$. If this difference is negative, the summary transverse force pushes the curved element towards the arched side, and the curvature increases until the tension (increased due to the elongation of the curved tube) becomes equal to the pressure-related force everywhere along the tube: $T = P\pi R^2$. So the minimum preliminary longitudinal tension for the straw T_0 in the detector frame may be evaluated from the condition $T_P = T_0 - (1 - 2\mu_\perp(E_\parallel/E_\perp))P\pi R^2 > 0$. One can conclude that the very minimum preliminary tension should be

$$T_0 = \left(1 - 2\mu_\perp \frac{E_\parallel}{E_\perp}\right) P\pi R^2, \tag{13}$$

where $P = 1$ at for straws filled with gas under atmospheric pressure and surrounded by vacuum. For safety the preliminary tensile force is usually made few times higher, as one needs to take into account the tension variance for different straws and some possible time-dependent loss of tension. It is limited mainly by straw strength as well as by rigidity of the frame.

Earlier the stability condition (13) has been derived for isotropic material in [11] using the analogy with an elastic rod buckling. The author of [11] considered a straw with free straw ends closed by airtight end plugs as an elastic rod. For the conditions of experiment [1], when straw ends are fixed, such a rod is compressed from the ends in order to eliminate its elongation (5). And the compressing force must be compensated by the preliminary straw tensile stress: $T_0/(2\pi RhE) = (1 - 2\mu)PR/(2hE)$, otherwise the compressed rod becomes transversely unstable and a buckling happens. But our present derivation of (13) is more general as it does not depend on any analogy.

Another consequence of the transverse force defined by the effective tension T_P is the prediction of oscillation lowest frequency for a long straw with some relatively small radius that may be regarded as a string. For transverse dynamics of a straw under pressure, the effective tension T_P plays the role of the usual string tension force. So one can derive the wave equation for a long straw with a pressure inside:

$$\frac{d^2y}{dt^2} = \frac{T_P}{\rho}\frac{d^2y}{dx^2}, \tag{14}$$

where ρ is the straw linear density; x is the longitudinal coordinate along the straw; and y is the transverse deviation of its axis.

Usual solution with the boundary conditions at the fixed ends gives the frequencies f spectrum:

$$f = \frac{n}{2L}\sqrt{\frac{T_0 - (1 - 2\mu_\perp \frac{E_\parallel}{E_\perp})P\pi R^2}{\rho}}. \tag{15}$$

Here n is a positive integer value and L is the straw length. So the lowest frequency oscillations of the tube under inner pressure are defined by the standard string formula with a usual tension replaced by the pressure-dependent effective tension T_P. The length of the tube on the testbench is defined by the movable support position as well as by the end cup C place. End cup mass is big enough to almost fix the straw end for the transverse oscillations.

Results of the lowest frequency measurements and their predictions (15) for $n = 1$ are shown in Fig. $3, b$. The straw elongation factor $(1 + T_0/E_\parallel 2\pi Rh)$ defined by the initial tension, that was applied during the support positioning, is taken into account both for L and ρ.

The prediction based on (15) seems to be deviated from the measurement results by up to 1 Hz. But the measurement uncertainty is not better than 1 Hz due to the observed widths of the spectrum peaks. Moreover, even for the tested small frequencies the testbench may be not rigid enough, and extra degrees of freedom (for example, end cup oscillations) may distort the simple straw oscillations spectrum. But the qualitative description seems to be achieved. So in practice, after the proper calibration, the frequency measurement procedure may be used for the straw effective tension diagnostics.

CONCLUSIONS

A new technique of mechanical properties study for straw tubes subjected both to inner pressure and longitudinal tension has been tested by means of the simple testbench that may be improved in future in order to avoid the transverse effect of gravitation.

A combination of parameters $\mu_\perp(E_\parallel/E_\perp)$ for Hostaphan® film is measured for two different straw specimens. Formulae derived to describe the observed experimental results may be used in order to predict the tension of gas-filled tube in vacuum.

It is found that a reaction of straw tube to a small local curvature is defined by the effective tension, that is the difference between the longitudinal wall tension and the pressure force applied to the cross section area of the tube. In particular, straw conserves its straightness only if this difference is positive. This defines a theoretical minimum axial tension that should be applied to the straw tube prior to air evacuation from the surrounding volume. Measurement of straw oscillation spectrum may be used for a straw tube effective tension estimation.

REFERENCES

1. *F. Hahn et al.*, Na62: Technical Design Document, Tech. Rep., CERN, Geneva, na62-10-07 (2010). URL https://cds.cern.ch/record/1404985/files/NA62-10-07.pdf
2. *A. Buonaura*, SHiP: A New Facility with a Dedicated Detector for Studying ν_τ Properties and Nucleon Structure Functions, PoS DIS2016 (2016) 260. arXiv:1609.04860.
3. *S. Timoshenko, S. Woinowsky-Krieger*, Theory of Plate and Shells, McGraw-Hill Book Co, International Edition, 1959.
4. *V. Davkov, K. Davkov, V. V. Myalkovskiy, V. Peshekhonov*, High Pressure Thin-Wall Drift Tubes, Instrum. Exp. Tech. 51 (2008) 787–791. doi:10.1134/S002044120806002X.
5. Vishay Precision Group, Inc., Single-Point Aluminum Load Cell. Model 1022. Tedea-Huntleigh. (2016). URL http://www.vishaypg.com/docs/12007/1022.pdf
6. MITSUBISHI POLYESTER FILM GmbH, Hostaphan RNK 2600 (2016). URL https://www.m-petfilm.de/wp-content/uploads/RNK_2600e.pdf
7. *F. James, M. Roos*, MINUIT: A System for Function Minimization and Analysis of the Parameter Errors and Correlations, Comput. Phys. Commun. 10 (1975) 343–367. doi:10.1016/0010-4655(75)90039-9.
8. *R. Brun, F. Rademakers*, ROOT: An Object Oriented Data Analysis Framework, Nucl. Instrum. Meth. A389 (1997) 81–86. doi:10.1016/S0168-9002(97)00048-X.
9. Goodfellow Group of Companies, Polyethylene Terephthalate (Polyester, PET, PETP) (2016). URL http://www.goodfellow.com/E/Polyethylene-terephthalate.html
10. DuPont Teijin Films, Mylar Polyester Film. Product Information. (2016). URL http://usa.dupontteijinfilms.com/informationcenter/downloads/Physical_And_Thermal_Properties.pdf
11. *D. C. Livio*, Qualification of the Longitudinal Weld of Thin Wall PET Tubes of the Straw Tracker of the Na62 Experiment, Master's Thesis, Haute Ecole Libre Mosane, Liege (2011).

Received on April 14, 2017.

Редактор *Е. И. Крупко*

Подписано в печать 1.06.2017.
Формат 60 × 90/16. Бумага офсетная. Печать офсетная.
Усл. печ. л. 0,93. Уч.-изд. л. 1,36. Тираж 255 экз. Заказ № 59128.

Издательский отдел Объединенного института ядерных исследований
141980, г. Дубна, Московская обл., ул. Жолио-Кюри, 6.
E-mail: publish@jinr.ru
www.jinr.ru/publish/